COMPUTATIONAL MODELLING OF THE TRANSPORT PHENOMENONS DURING LOW TEMPERATURE IN-BIN DRYING AND AERATION OF AMARANTH GRAINS

Ana M. Pagano[a,c] and Rodolfo H. Mascheroni[b,c]

[a]Núcleo TECSE, Depto. Ingeniería Química, Facultad de Ingeniería, Universidad Nacional del Centro de la Provincia de Buenos Aires (UNCPBA), Av. del Valle 5737, 7400 Olavarría, Argentina, apagano@fio.unicen.edu.ar, http://www.fio.unicen.edu.ar

[b]Centro de Investigación y Desarrollo en Criotecnología de Alimentos (CIDCA), CONICET La Plata, -UNLP, rhmasche@ing.unlp.edu.ar

[c]MODIAL, Facultad de Ingeniería, Universidad Nacional de La Plata (UNLP), Calle 47 y 116, (1900) La Plata, Argentina, http://www.ing.unlp.edu.ar

Keywords: Amaranth, in-bin drying, grain aeration, computational mechanics, modeling.

Abstract. In the present work a full model for the in-bin low-temperature drying of amaranth grains based on the finite elements method (FEM) was developed, taking into account re-analyzed specific relationships developed in previous works for description of properties of grains, drying kinetic and equilibrium moisture content. Due to the nature and symmetry of the problem of in-bin drying and aeration of amaranth grains, FEM model was performed considering a one-dimensional domain. The discretization was made through a structured mesh density having 96 Lagrange quadratic elements. Coupled One-Dimensional Transport Equations for Moisture Mass, Heat and Momentum Transfer in both phases (solid and gas) were planned and solved using the following Application Modes of COMSOL Multiphysics® 3.5a: transient analysis of Convection and Diffusion (for air and grain) from Multiphysics Module; transient analysis of General Heat Transfer (for air and grain) from the Heat Transfer Module; and state analysis of fluid flow with Darcy´s Law (for air) from the Earth Science Module. The grain bed was considered unique-like material with effective properties (i.e., diffusivity, permeability). Experimental data and relationships of thermo-physical properties, equilibrium moisture content, heat of sorption, drying kinetics and resistance to airflow determined in previous works were used to define the Constants, Scalar and Global Expressions in the definition of the COMSOL FEM model. Voids fractions and superficial velocities were specified, and pressure-drops through the grain bed, and rates of heat and mass transfer from the kernels to the air, were determined. The simulations of the FEM model provided useful information about temporal and spatial moisture content in the deep bed of amaranth grains.

1   INTRODUCTION

Grains are usually harvested in high moisture, being then dried and stored in bins before processing. During the drying and storage periods with aeration, the ambient conditions can affect the grain quality. Drying/aeration grain quality depends on a suitable control of the operation´s parameters. Flow rate, temperature and relative humidity of the drying air play an important role in these postharvest processes.

In convective air drying of grains, two distinct transport mechanisms occur simultaneously, involving heat transfer from the drying air to the kernel and water transport from the interior of the solid product to its surface, and eventually to the air through evaporation (Sabarez, 2012). The heat and mass transfer rates depend on both temperature and concentration differences as well as on the air velocity field.

The simulation of grain drying systems involves solving a set of heat and mass transfer equations which describe the heat and moisture exchange between product and air, the adsorption and desorption rates of heat and moisture transfer, the equilibrium relations between product and air, and the psychometric properties of moist air (Gavrila et al. 2008).

These considerations lead to complex partial differential equations for the moisture content and temperature fields inside the product. These equations incorporate transport coefficients which must be determined experimentally, and are strong functions of moisture content and temperature (Gavrila et al. 2008).

Numerous theoretical models have been proposed to simulate the deep bed drying of grains. These models can be classified into non equilibrium, equilibrium and logarithmic models. The first group describes the condition of non equilibrium between the air and the grain by mean of partial differential equations (PDE). The other two groups of models are simplifications of the non equilibrium models with some assumptions related to the boundary conditions to reduce the complexity and calculus time, however, this compromise regarding boundary conditions reduces the prediction accuracy of the models. On the other hand, non equilibrium models -developed using a set of PDEs with minimal assumptions- are detailed, accurate, and valid for grain drying (Zare et al. 2012).

Between semiempirical models, Thompson et al. (1968) proposed a grain drying model for solving the mass and energy balances considering the thickness of the grain mass as constructed by thin layers of a grain diameter thickness, placed one above the other. From knowledge of the drying behavior of a thin layer, by means of the energy and mass balances, the deep bed drying can be studied using an iterative process. These authors considered the deep bed of grain as a series of overlapping thin layers of grain, where drying temperature and the relative humidity of the outlet air from any layer is the input to the next (Jia, 2002; Cubillos Varela and Barrero Mendoza, 2010).

The PDE model for solving the energy and mass balances consists of four partial differential equations, containing four unknowns in the model, namely, drying air temperature and humidity, grain temperature and moisture content. The set of PDEs cannot be solved by analytical methods and requires numerical solutions and computer programming to allow the prediction of the grain moisture content at various locations (depths) in the drying chamber at any instant (Zare et al. 2012). Between them, the method of finite elements constitutes a valuable tool (Haghighi and Segerlind, 1988; Lund, 2009; Gavrila et al. 2008; Fortes et al. 2009).

Many researches on the mathematical modeling and actual studies have been conducted on the thin layer and deep bed drying processes of various agro-based products (Milojevića and Stefanović, 1982; Brooker et al. 1992; Abalone et al. 2006; Aregba and Nadeau, 2007; Lund, 2009; Stakić et al. 2011; Zare et al. 2012; Martinello et al. 2013); however, very little

information is available on deep bed drying and modeling for amaranth seeds (Abalone et al. 2006; Ronoh et al. 2009).

In order to reduce losses in the field, amaranth grains are harvested with a moisture content of approximately 30% dry basis (or more), and subsequently must be necessarily exposed to applying artificial drying to reduce the moisture level below 10% dry basis approximately, to ensure safe storage (Abalone et al. 2006; Ronoh et al. 2009; Li, 2011).

Therefore, this study was performed to develop a numerical PDE model for deep bed drying grain amaranth based on an appropriate set of thermo-physical and equilibrium properties, and kinetics of thin-layer drying, in order to predict the moisture, temperature and pressure profiles and gradients during drying.

In this paper, a mathematical model was developed to describe the coupled heat, mass and momentum transfer processes occurring in convective drying of deep-bed amaranth grains. Grain bed is represented as a composite material having effective properties. The model accounts the variation of both air and grain properties expressed as a function of temperature and moisture content. The resulting systems of transient non-linear partial differential equations (PDEs) in the space–time domain together with the set of initial and boundary conditions were numerically solved by applying the finite element method (FEM) using a commercial package (COMSOL Multiphysics®).

2 PRELIMINARY DATA AND METHODOLOGY OF APPROACH

The amaranth grain was assumed as a homogeneous and isotropic material, without shrinkage during drying. The irregular grain shape was approximated through a revolution volume resulting by the union of two ellipsoids. The characteristics lengths of the particle and the thermo-physical properties of the grain and drying air were determined by the following information.

2.1 Properties of grain and air

Equivalent diameter of the particle

The equivalent diameter (D_{eq}, m) of a sphere with the same volume that an amaranth grain was correlated with the initial moisture content through the following equation (Abalone et al. 2004; Pagano and Mascheroni, 2011):

$$D_{eq} = 10^{-3}\left(0.987 + 0.00341 M_0\right)$$

(1)

where M_0: initial moisture content (% d.b.).

Grain and bulk density, bed porosity

The grain and bulk densities and the bed porosity were predicted based on the initial moisture content by the equations (Abalone et al. 2004) showed next:

$$\rho_g = \frac{1411\left(100 + M_0\right)}{\left(100 + 1.25 M_0\right)}$$

(2)

$$\rho_b = \left(869 - 3.50 M_0\right)$$

(3)

$$\varepsilon = \left(0.38 + 0.0016 M_0\right)$$

(4)

where ρ_g: grain density (kg/m^3); ρ_b: bulk density (kg/m^3); ε: bed porosity (decimal).

Density of dry solid

The density of the dry solid (ρ_s) was evaluated considering the densities of the amaranth grain components (65.1% carbohydrates; 12.9% proteins; 7.2% lipids; 6.7% fibers; 2.5% ash) (FAO, 1999) applying the following expression (Choi and Okos (1986) in Ibarz-Ribas and Barbosa-Cánovas, 2005):

$$\rho_s = \frac{1}{\sum\limits_i \left(\dfrac{x_i^m}{\rho_i} \right)}$$

(5)

where x_i^m: mass fraction of the component i; and ρ_i: density of that component (kg/m^3).

The densities of the amaranth grain components were estimated by the corresponding correlations shown in Table 1 in function of the temperature.

Thermal conductivity

On the same sense, the thermal conductivity of the grain (k_g) was estimated using the next equation (Ibarz-Ribas and Barbosa-Cánovas, 2005):

$$k_g = \sum\limits_i \left(k_i x_i^V \right)$$

(6)

where k_i: thermal conductivity of component i (W/(m K)); and x_i^V is the volume fraction of that component. The volume fraction of component is given by:

$$x_i^V = \frac{x_i^m / \rho_i}{\sum\limits_i \left(\dfrac{x_i^m}{\rho_i} \right)}$$

(7)

The thermal conductivity of each of the components of the grain was estimated from the equations presented in Table 1 proposed by Choi and Okos (1986) (in Ibarz-Ribas and Barbosa-Cánovas, 2005) to calculate k_i for each component of the material, in function of the drying temperature (in ºC).

Specific heat and thermal diffusivity

Also, the mean specific heat of the solid (C_{pg}) and the thermal diffusivity (α) were calculated in function of drying temperature by the following relationships (Choi and Okos, 1986, in Ibarz-Ribas and Barbosa-Cánovas, 2005), as average of the individual grain components included in their centesimal composition (Mujica Sánchez et al. 1999). The effective specific heat for grain bed was evaluated as $C'_{pg} = (C_{pg} + C_{pw} M_{dec})$ J/(kg K), being M_{dec} the decimal grain moisture content in dry basis (Lund, 2009).

Air and water vapor properties

The air and water vapor properties were evaluated at the drying temperature: air thermal conductivity $k_a = 0.03$ W/(m K); air density $\rho_a = 1.2$ kg/m^3; specific heat of dry air $C_{pa} = 1000$ J/(kg K); air viscosity $\mu_a = 2 \times 10^{-5}$ (Pa s); specific heat of liquid water $C_{pw} = 4100$ J/(kg K)

(Coronel Toro, 2005; Lund, 2009); effective specific heat for drying air $C'_{pa} = (C_{pa} + C_{pw} \, o_m)$ J/(kg K), being o_m the absolute humidity of air (kg water-vapor/kg air); moisture diffusivity in air $D_a=2.6\times10^5$ m²/s (Lund, 2009).

Property	Component	Expression	Eq.
thermal conductivity W/(m K)	carbohydrate	$0.20141 + 1.3874\times10^{-3}\,T - 4.3312\times10^{-6}\,T^2$	(8)
	ash	$0.32962 + 1.4011\times10^{-3}\,T - 2.9069\times10^{-6}\,T^2$	(9)
	fiber	$0.18331 + 1.2497\times10^{-3}\,T - 3.1683\times10^{-6}\,T^2$	(10)
	lipid	$0.18071 + 2.7604\times10^{-3}\,T - 1.7749\times10^{-6}\,T^2$	(11)
	protein	$0.17881 + 1.1958\times10^{-3}\,T - 2.7178\times10^{-6}\,T^2$	(12)
	water	$0.57109 + 1.7625\times10^{-3}\,T - 6.7036\times10^{-6}\,T^2$	(13)
specific heat J/(kg K)	carbohydrate	$1548.8 + 1.9625\,T - 5.9399\times10^{-3}\,T^2$	(14)
	ash	$1845.9 + 1.8306\,T - 4.6509\times10^{-3}\,T^2$	(15)
	fiber	$1092.6 + 1.8896\,T - 3.6817\times10^{-3}\,T^2$	(16)
	lipid	$1984.2 + 1.4733\,T - 4.8008\times10^{-3}\,T^2$	(17)
	protein	$2008.2 + 1.2089\,T - 1.3129\times10^{-3}\,T^2$	(18)
	water	$4176.2 - 9.0864\times10^{-2}\,T + 5.4731\times10^{-3}\,T^2$	(19)
density kg/m³	carbohydrate	$1599.1 - 0.31046\,T$	(20)
	ash	$2423.8 - 0.28063\,T$	(21)
	fiber	$1311.5 - 0.36589\,T$	(22)
	lipid	$925.59 - 0.41757\,T$	(23)
	protein	$1329.9 - 0.5184\,T$	(24)
	water	$997.18 + 0.0031439\,T - 0.0037574\,T^2$	(25)
thermal diffusivity ($\times10^6$), m²/s	carbohydrate	$8.084\times10^{-2} + 5.305\times10^{-4}\,T - 2.3218\times10^{-6}\,T^2$	(26)
	ash	$1.246\times10^{-1} + 3.732\times10^{-4}\,T - 1.2244\times10^{-6}\,T^2$	(27)
	fiber	$7.398\times10^{-2} + 5.190\times10^{-4}\,T - 2.2202\times10^{-6}\,T^2$	(28)
	lipid	$9.878\times10^{-2} + 1.257\times10^{-4}\,T - 3.8286\times10^{-8}\,T^2$	(29)
	protein	$6.871\times10^{-2} + 4.758\times10^{-4}\,T - 1.4646\times10^{-6}\,T^2$	(30)
	water	$1.317\times10^{-1} + 6.248\times10^{-4}\,T - 2.4022\times10^{-6}\,T^2$	(31)

Table 1. Equations for calculating some thermal and physical properties of components of amaranth grain (Ibarz-Ribas and Barbosa-Cánovas, 2005).

2.2 Transport coefficients

The coefficients of mass transfer (h_m, m/s) and heat transfer (h, W/(m² ºC)) were obtained from the following correlations (Masciarelli et al. 2012; Lopez, 2011):

$$h_m = ShD_a / D_{eq} \qquad \text{with } Sh = 2 + 0.6Rê^{1/2}Sc^{1/3} \tag{32}$$

$$h = NuD_{eq} / k_g \qquad \text{with } Nu = 0.37Re^{0.6} \tag{33}$$

2.3 Equilibrium moisture content of grains and heat of desorption

The equilibrium moisture content of grains was estimated by means of the following expression of the generalized GAB model with one of their parameters depending on temperature (Pagano and Mascheroni, 2003b, 2003c; 2005):

$$M_e = \frac{2.6288 \times 10^{-4} \exp\left(\frac{32325}{R_g(T_a + 273)}\right) a_w}{\left(1 - 0.7034 a_w\right)\left(1 - 0.7034 a_w + 3.8265 \times 10^{-5} \exp\left(\frac{32325}{R_g(T_a + 273)}\right) a_w\right)} \tag{34}$$

where M_e: equilibrium moisture content (% d.b.); R_g: 8.314 J/(mol K); T_a: air temperature (ºC); a_w: water activity.

The heat of desorption of water from amaranth was evaluated in function of the moisture content of grains and temperature, based on applying the next correlation of the net heat of desorption (Pagano and Mascheroni, 2003a) plus the vaporization enthalpy of the free water ($hfg = hfg_n + hfg_w$) (Sun et al. 1995):

$$hfg_n = 384316.7 R_g 0.8111^{M_e} \tag{35}$$

$$hfg_w = 3152036 - 2384.1(T_a + 273) \tag{36}$$

where hfg_n: net heat of desorption (J/kg); hfg_w: enthalpy of vaporization of free water (J/kg).

2.4 Single-kernel drying kinetics data

In a previous work (Pagano and Mascheroni, 2011), the thin-layer drying of amaranth grains was experimentally studied for temperatures from 25 to 70ºC and initial moisture contents between 15 and 32.5% d.b. (dry basis), modeling the experimental data by the theoretical model of "short times" based on the Fick´s law (Becker, 1959), and describing the kernels shape by means of different geometrical interpretations: sphere, oblate ellipsoid and volume of revolution. The diffusion coefficient of moisture estimated for these shape characterizations of grains were determined. From these results, the diffusion coefficient was expressed by an Arrhenius type dependence with the reciprocal of the absolute temperature, and a linear function of initial moisture content of grain were probed, resulting mean activation energy of 25.1 kJ/mol.

$$D_{ef} = \left(2.151 \times 10^{-8} + 1.791 \times 10^{-6}(M_0 - 0.149)\right) \exp\left(\frac{-\overline{E_a}}{R_g T_a}\right) \tag{37}$$

where $\overline{E_a}$: mean activation energy (J/mol).

Also in that work, numerical 2D FEM models performed in ANSYS® were developed for solving the mass transfer equation that describes the experimental drying of individual grains, by analogy with the problem of thermal diffusion; grain surface instantaneously attaining

equilibrium moisture content (strict internal control during the drying process) was assumed as boundary condition. The best description of drying curves was obtained when the domain was modeled by a 2D ellipsoidal geometry applying moisture diffusion coefficient of spheres, which were between $1.85 \times 10^{-12} - 5.19 \times 10^{-11}$ m^2/s.

The moisture diffusivity usually falls in approximately 10^{-11} m^2/s for grains dried at moderate temperatures (Lund, 2009; Ibarz-Ribas and Barbosa-Cánovas, 2005), whereas the thermal diffusivity is usually of about $\alpha \approx 10^{-8}$ m^2/s. From the above reference of amaranth grains drying, the ratio (α/D_{ef}) resulted from between 5.3×10^2 and 3.7×10^4. That is, thermal diffusivity α was between 2 and 4 orders higher than the effective moisture diffusivity D_{ef}, which means that heat diffusion is much faster than the mass diffusion, hence the grain temperature may be assumed virtually equal to that of the drying air, as was probed by Pagano and Mascheroni (2011).

However, the effect of convection was not considered in mentioned work when solving the equation of mass transfer. The effect of the grain characterization on the accuracy of the models has not been investigated neither by two-dimensional nor by three dimensional domains.

In literature, most numerical simulations reported for drying grains were conducted based only on 2D FEM models. For the amaranth grains, there is no information reported that simultaneously solves either two-dimensional (2D) and three-dimensional (3D) transient temperature and moisture fields during drying.

In virtue of this, in the present work it was speculated that since an amaranth grain has an irregular geometrical shape, a 3D FEM model on the coupled heat and mass transfer for the drying of a single amaranth grain could be expected to increase the accuracy of simulation as compared to a 2D simulation. This model would be able to provide useful information for the drying simulation of grains in deep bed.

3 DEVELOPMENT OF A 3D FEM MODEL FOR SINGLE-KERNEL DRYING

As was anticipated, in a previous experimental study of the thin-layer drying of amaranth grains based on two-dimensional FEM models (Pagano and Mascheroni, 2011), it was found that the best geometrical approach to describe the kernel shape subjected to drying corresponded to an oblate ellipsoid. Notwithstanding, the domain property related with the diffusion coefficient must be set as the diffusivity of a sphere with the same volume that corresponding to the oblate ellipsoid.

For the purpose of developing a more consistent (and if possible, more precise) description of individual grain drying amaranth to obtain the information necessary for deep bed drying, a new three-dimensional numerical model with a geometry analogous to grain was proposed. This model was defined in COMSOL Multiphysics® 3.5a to solve the simultaneous mass and heat transfer phenomena comparatively with the mentioned previous work.

Governing equations

The 3D modeling of single-kernel drying was made based on the following assumptions:
- Amaranth grain shape is a volume revolution resulting of the superposition of two concentric ellipsoids (Fig. 1).
- Unsteady heat conduction and moisture diffusion take place within the kernel.
- Only convective heat and mass transfer takes place between the kernel surface and its drying environment.
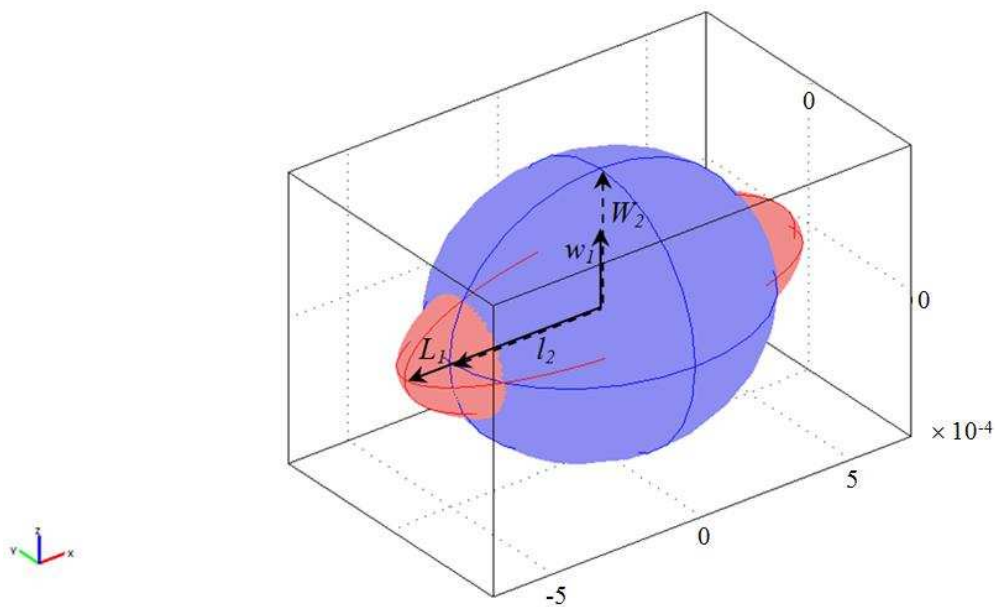
Figure 1. Physical domain in the Cartesian coordinate system (x: length direction; y: width direction; z: thickness direction, being width=thickness; L_1, w_1: major and minor semi-axis of the pink ellipsoid, respectively; l_2, W_2; major and minor semi-axis of the blue ellipsoid, respectively).

Based on the above assumptions, the 3D governing equations in a Cartesian coordinate system (x, y, z) were expressed as (Crank, 1964; Holman, 1976; Wu et al. 2004):

$$\rho_g C_{pg} \frac{\partial T_g}{\partial t} = k_g \left(\frac{\partial^2 T_g}{\partial x^2} + \frac{\partial^2 T_g}{\partial y^2} + \frac{\partial^2 T_g}{\partial z^2} \right) \tag{38}$$

$$\frac{\partial M}{\partial t} = D_{ef} \left(\frac{\partial^2 M}{\partial x^2} + \frac{\partial^2 M}{\partial y^2} + \frac{\partial^2 M}{\partial z^2} \right) \tag{39}$$

where T_g: temperature (ºC); M: moisture content of grain (% d.b.); t: time (s).

Boundary and initial conditions

For t>0 and at the grain surface:

$$- D_{ef} \frac{\partial M}{\partial n} = h_m (M - M_e) \tag{40}$$

$$- k_g \frac{\partial T}{\partial n} = h (T_g - T_a) \tag{41}$$

When   t=0:   M= M_0, T_g= T_{g0} (42)

where n: normal to kernel surface; T_a: air temperature surrounding the grain, T_g drying temperature, (ºC); T_{g0}: initial temperature of the grain (ºC).

It should be noted that D_{ef}, k_g, ρ_g and C_{pg} change with kernel temperature, moisture content, and different layers in the kernel, while h_m, h and M_e change with the drying medium temperature, air velocity and relative humidity. The formulae of those parameters have been precedently mentioned.

Domain definition and discretization

In virtue of the symmetry of the problem, only a quarter of an amaranth grain was taken as domain to simulate the convective drying at different conditions (initial moisture contents: 15-32.5% d.b.; drying temperatures: 25-70°C; air velocities: 0.3-3 m/s).

The length semiaxis (L_1, w_1, l_2, W_2) of both concentric ellipsoids used to describe the amaranth grain (Fig. 1) were determined in function of the initial moisture content by the following relationships (Abalone et al. 2004). The thicknesses were considered equal to the widths for both ellipsoids.

$$L_1 = 10^{-3}(0.625 + 0.00203 M_0) \tag{43}$$

$$w_1 = 10^{-3}(0.231 + 0.00098 M_0) \tag{44}$$

$$l_2 = 10^{-3}(0.481 + 0.00157 M_0) \tag{45}$$

$$W_2 = 10^{-3}(0.393 + 0.00168 M_0) \tag{46}$$

The domain was automatically meshed using 30919 quadratic tetrahedral elements of Lagrange with 89632 degrees of freedom. Convergence of results in function of mesh density was analyzed. The coupled equations of mass and heat transfer (Eq. 38 and 39) for single-kernel drying were solved by mean of a transient analysis performed in COMSOL Multiphysics® 3.5a with the Modules Convection and Diffusion, and Convection and Diffusion of Heat Transfer corresponding to the COMSOL Multiphysics Application Mode.

Transport coefficients

From the correlations showed in Eq. (32) and (33), the mass transfer coefficient resulted of about $h_m \approx 0.06$ for the experimental condition air velocity $V_a = 0.3$ m/s, drying temperature of $T_a = 35$°C, initial moisture content of amaranth grains $M_0 = 15\%$ d.b.

As result of this, the Biot number for mass transfer Bi_m were of about 10^7, while the corresponding Biot number to heat transfer Bi close only in two digits, evidencing that the drying process in controlled by internal mass diffusion and by external heat convection.

The mass and heat transfer coefficients (h, h_m) were used as data input in the definition of the convective boundary conditions of the Convection and Diffusion and Convection and Conduction Modules of the Modes Convection and Diffusion, and Heat Transfer of COMSOL Multiphysics® 3.5a.

Model resolution

The system was solved with the Direct SPOOLES Solver for transient analysis, and results of spatial and temporal distribution of moisture content and temperature were obtained. As example, Fig. 2 shows a slices graph of moisture content for two particular conditions, while Figs. 3 and 4 present the temperature and moisture profiles at different drying times. Similar graphs resulted for the other experimental cases.
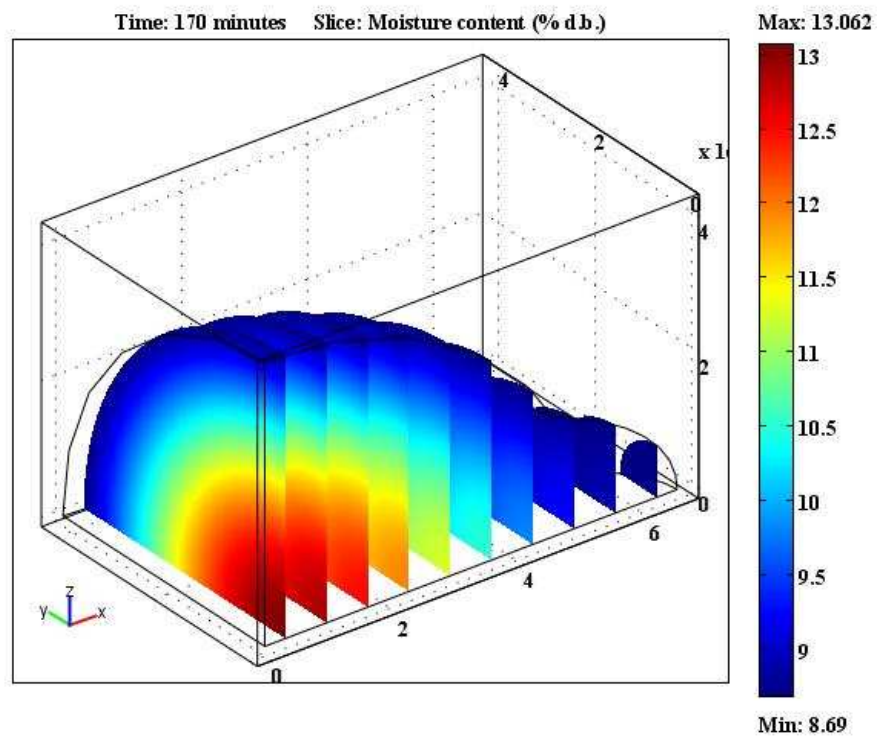
(a)
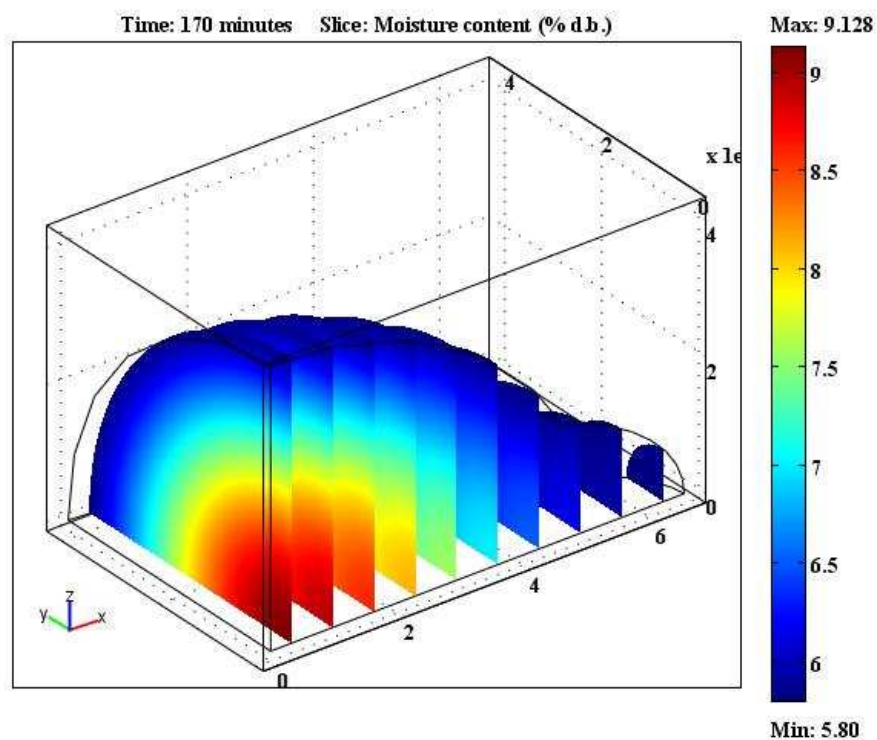
(b)

Figure 2. Slices graphs of moisture content distribution in amaranth grain at 170 minutes drying time for the experimental conditions: M_0=15% d.b.; V_a=0.3 m/s; a) T_a =35ºC; b) T_a=55ºC.
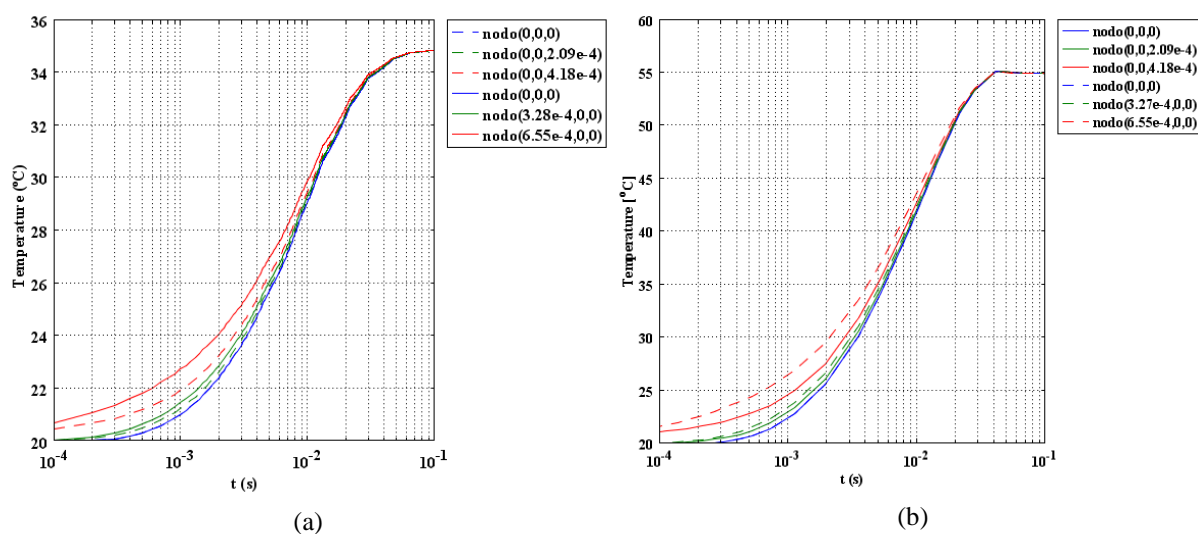
Figure 3. Temporal temperature profiles inside the amaranth grain during drying at some nodes located on the x-length direction (solid lines) and on the z-width direction (equal to y-thickness direction) (dashed lines) for the experimental conditions: M_0=15% d.b.; V_a=0.3 m/s; a) T_a =35ºC; b) T_a =55ºC.
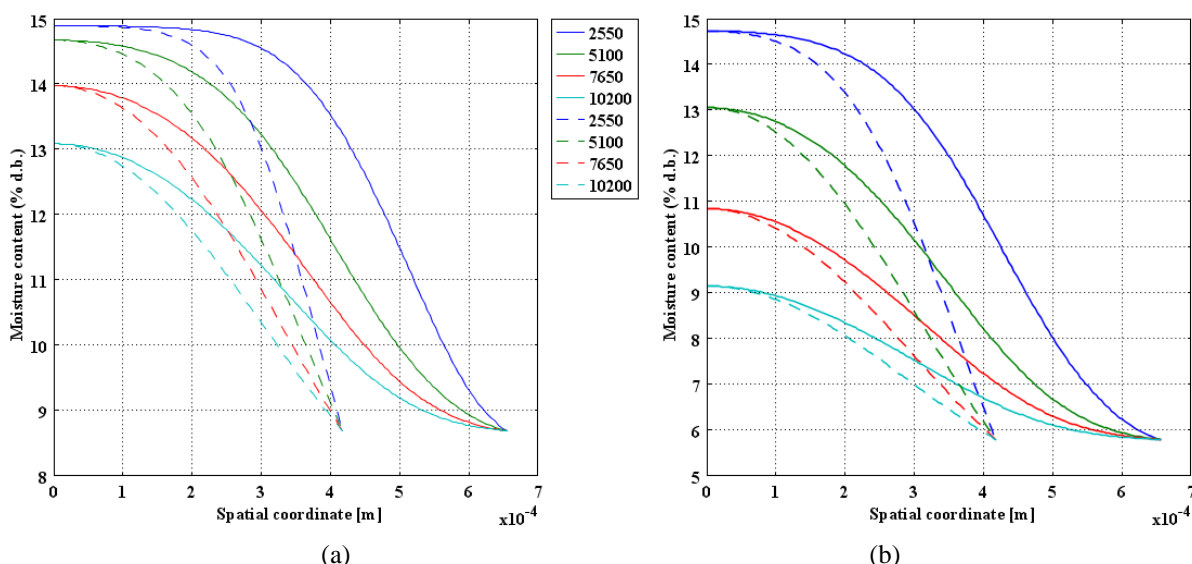
Figure 4. Spatial moisture content profiles inside the amaranth grain at several instants (2550, 5100, 7650 y 10200 s) during drying in the x-length direction (solid lines) and in the z-width direction (equal to y-thickness direction) (dashed lines) for the experimental conditions: M_0=15% d.b.; V_a=0.3 m/s; a) T_a =35ºC; b) T_a=55ºC

It is clear that the thermal equilibrium is quickly reached in a few seconds while, opposite this, great gradients of moisture still remain in the amaranth grain, yet after several minutes (even hours) of drying. This behavior would allow simplify the coupled problem, being independent from the temperature which remains virtually constant throughout the process.

The performance of the 3D convective model to describe the pool of measured data of grain moisture content in function of drying time (from Pagano and Mascheroni, 2011) was clearly better than the 2D previous models (Pagano and Mascheroni, 2011), such as can be observed in Fig. 5 for one particular experimental condition, except only in the very early phase of the drying process, generally less important than the final stage, that defines the required time to reach the security moisture grain.
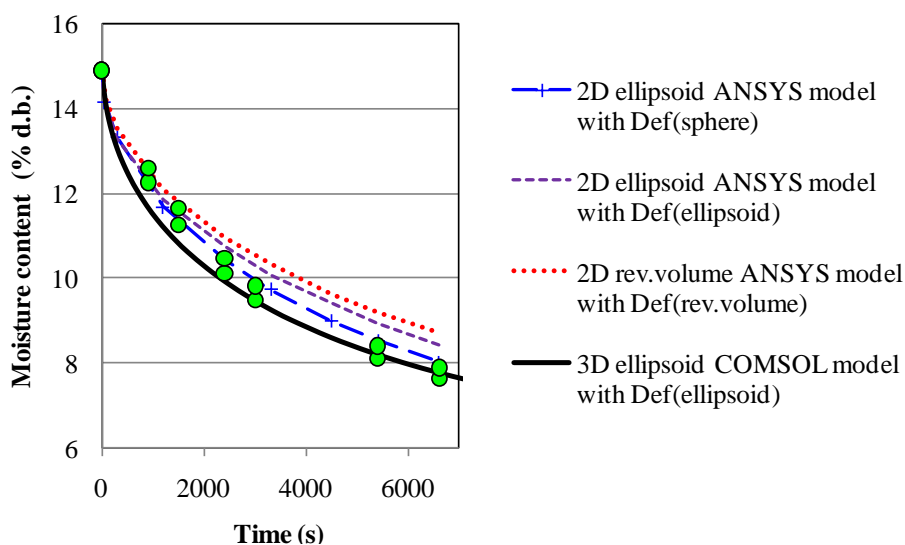
Figure 5. Experimental drying data (green points) and predicted curves of 3D COMSOL model (solid black line) and 2D ANSYS model (Pagano and Mascheroni, 2011) for amaranth grains dried at the conditions: $M_0=15\%$ d.b.; $T_a=55ºC$, $V_a=0.3$ m/s.

On this basis, the single kernel 3D model validated here was extended to volumetric mass transfer in a bed of static amaranth grains having specified constant void fraction (porosity).

For that, scaled variables $MR=(M-M_e)/(M_0-M_e)$ and $\tau=t/t_k$ were introduced (where $t_k=D_{eq}^2/D_{ef}$, kernel moisture time constant) in order to determine a moisture volume-average concentration according to the procedure proposed by Lund (2009). When the volumetric average concentration and its time derivative were computed by COMSOL, the following dimensionless curves (Fig. 6) were obtained in a semi-logarithmic graph.
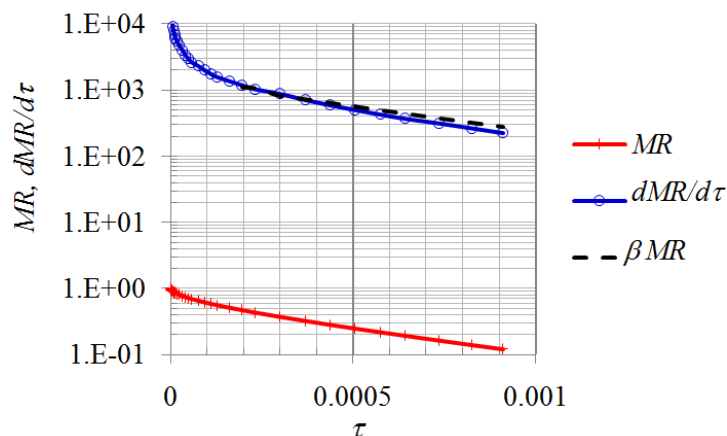
Figure 6. Grain average moisture concentration obtained from the 3D COMSOL model for amaranth grains dried at the conditions: $M_0=15\%$ d.b.; $T_d=55ºC$, $V_a=0.3$ m/s.

Excluding very early data, both curves present decay exponentially and proportional to an approximately constant factor β, responding to the following correlation obtained by non-linear regression ($R^2>0.987$):

$$-\frac{d\overline{MR}}{d\tau} = \beta\overline{MR} \qquad ; \qquad \beta = \frac{(2235.45\tau - 0.5626)}{(\tau - 0.00025)} \qquad (47)$$

Taking the mean moisture transfer from one grain:

$$V_{1g} \rho_g \frac{d\overline{M}}{dt} = h_{mef} S_{1g} \rho_g \left(\overline{M} - M_e\right) \qquad (48)$$

where V_{1g}: volume of one grain (m^3); S_{1g}: surface area of one grain (m^2); h_{mef}: effective mass transfer coefficient (m/s).

From the comparison between Eqs. (47) and (48), the effective mass transfer coefficient h_{mef} can be obtained as:

$$h_{mef} = \frac{\beta D_{eq}}{6t_k} = \frac{2}{3} \frac{\beta D_{ef}}{D_{eq}} \qquad (49)$$

Average moisture transfer resulted in the order of 10^{-6} m/s showing dependency essentially internal diffusivity, such as been reported by Lund (2009) for wheat grain drying.

The mass transfer to the air (Q_m, kg/s) was extended to a bed of N grains and was a source term in the Convection and Diffusion Module in COMSOL Multiphysics® 3.5a, with equations solved as one-dimensional time-dependent (Lund, 2009), considering that:

$$Q_m = q_{Vm} V_T = N h_{mef} S_{1g} \rho_g \left(\overline{M} - M_e\right) = \left(1 - \varepsilon\right) \frac{V_T}{V_{1g}} h_{mef} S_{1g} \rho_g \left(\overline{M} - M_e\right) \qquad (50)$$

where q_{Vm}: volumetric mass transfer (kg/(s m^3)); V_T: total bed volume (m^3); N: number of grains.

4 PRESSURE DROP FOR FIXED DEEP-BED AERATION/DRYING

From the theoretical point of view, the problem of fluid flow in porous media is governed by the laws of conservation of mass, momentum and energy (Pagano and Mascheroni, 2010). Given the complexity involved in the analytical treatment of the phenomenon of flow in porous, often resorts to empirical evaluation and simplifications of the modeling are chosen. One of them is the Law of Darcy, applicable at low flow rates (laminar flow) where the resistance to movement of fluid friction is proportional to the fluid viscosity and velocity due to viscous forces predominate over inertial forces (Garg and Maier, 2006).

4.1 Analysis by the Finite Element Method (FEM)

Governing equations

In order to develop a numerical model to simulate the effect of a porous medium on the flow of a fluid, a convenient and simplified approximation that can be applied is to consider the particle packing as a distributed resistance in the geometry of the domain.

The resistance to fluid flow can be attributed to one or more factors in combination: localized losses (F), the friction factor (f) and/or related factor C permeability (K=1/C) (de Andrade et al. 2001). The total pressure gradient ($\partial P/\partial y$) consists of the sum of these three components, as outlined in the following equation, for example y-axis direction:

$$\frac{\partial P}{\partial y} = -\left\{ F\rho V_y |V| + \frac{f}{D_h} \rho V_y |V| + C_y \mu V_y \right\}$$
(51)

where D_h: hydraulic diameter (m); C_y: reciprocal bed permeability in the y-Cartesian direction (m^{-2}); μ: viscosity (Pa s); V: velocity (m/s).

In a previous work (Pagano and Mascheroni, 2010), the airflow resistance of the porous bed of amaranth grains was determined and modeled as a distributed resistance of the grain bed, assuming that this artificial imposed condition represents the average of the pressure drops through the porous bed. In that work, the non-uniform flow distribution in the grain bed was solved by the finite element method using the module FLOTRAN (computational fluid dynamics, CFD) of ANSYS® software, in steady state considering a 2D axial symmetrical geometry. The porous medium was considered isotropic due the amaranth grain sphericity close to unity (0.82) (Abalone et al. 2004), negligible friction losses at the walls of silo and localized pressure losses (de Andrade et al. 2001). By application of an optimization technique available in the commercial program ANSYS®, it was possible to determine the permeability of amaranth beds and get patterns for describing fluid flow in porous media. From the experimental determination of the airflow resistance of amaranth grains beds (Pagano and Mascheroni, 2010), the finite element model developed by this tool allowed to predict with great accuracy the values of the pressure drop across the bed to different packaging (loose fill and dense fill), bed heights and a wide range of air flow rates. For a bed depth of 0.14 m, these airflow resistances were from 94.4 to 351.9 Pa when airflow velocity varied between 0.03 and 0.11 m^3/s-m^2. Intrinsic permeability K of amaranth beds resulted between 7.693×10^{-10} and 9.142×10^{-10} m^2, being possible to correlate it with the flow velocity of air (V_a) through second order polynomial, as is shown in the following equation for loose bed (R^2=0.9).

$$K = -3 \times 10^{-8} V_a^2 + 2 \times 10^{-9} V_a + 9 \times 10^{-10}$$
(52)

These correlations were used to predict pressure drop in the amaranth grain exposed to low-temperature drying by means of a full numerical one-dimensional model for drying and aeration, which was performed in COMSOL Multiphysics® 3.5a, as will be detailed next.

Problem definition and domain discretization

For determining the pressure drop across the amaranth bed exposed to aeration, the *Darcy's Law* of Fluid Flow Module (stationary state pressure analysis) of the Earth Science Application Mode of COMSOL Multiphysics® 3.5a was used. The domain was defined as one-dimensional characterized by the bed height (L), and discretized with 96 Lagrange quadratic elements (Fig. 7) after analysis of the convergence of results. Physical property K calculated in function of the airflow rate was set as sub-domain coefficient.

Boundary and initial conditions

Boundary conditions of fixed inward flux (V_a, m/s) at the inlet of airflow and null pressure at the bed top were imposed; while P_0=0 was considered as initial condition.

The UMFPACK solver was used to fluid flow model resolution. Profiles of pressure along domain were obtained in the range of airflow velocities for loose and dense fill. Predictions of the airflow resistance of amaranth grains obtained by the 1D COMSOL model resulted coincident with experimental data and also concordant with estimations of the 2D ANSYS model obtained by Pagano and Mascheroni (2010), with the advantage of minor complexity

of 1D model. These results can be noted in Fig. 8 as example for loose bed; similar graphs were obtained for other conditions.
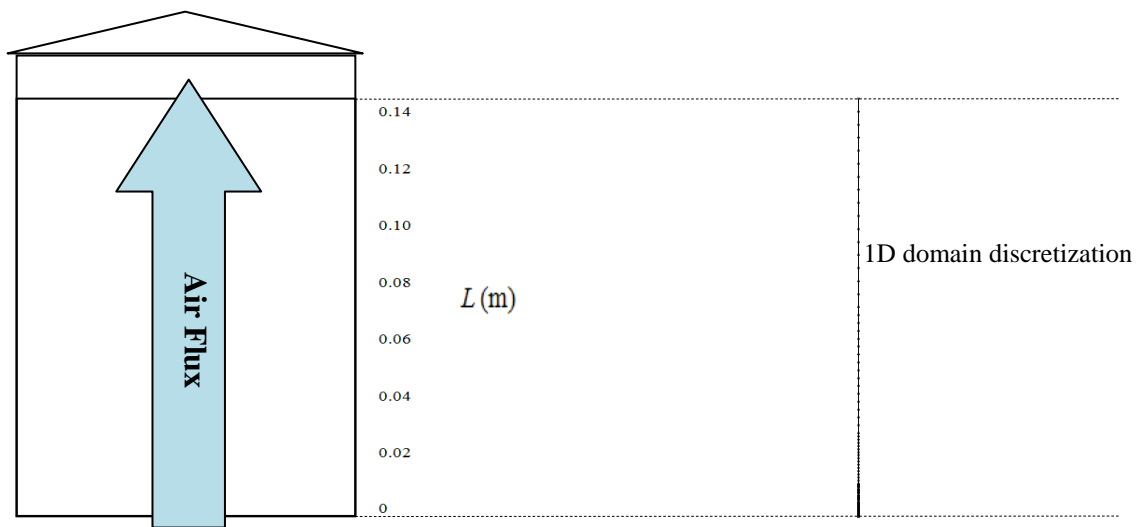
Figure 7. Scheme of the domain characteristics and discretization.
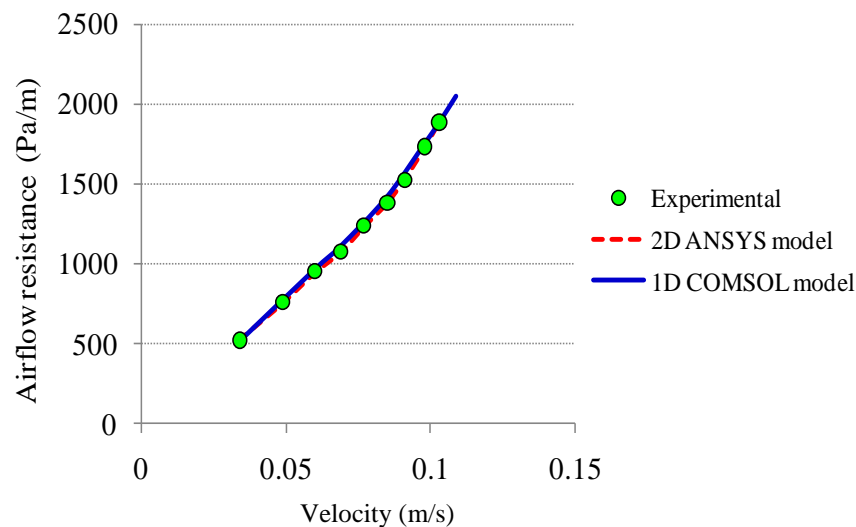
Figure 8. Experimental (points) of airflow resistance (or pressure drop per unit bed depth) of amaranth grains in loose beds at different airflow rates, compared with the predictions of the numerical 2D ANSYS (dashed red line) and 1D COMSOL (full blue line) models.

On basis of this study, with the same vision, the modeling approach of deep bed drying was planned, simplified to a single spatial dimension 1D for the further analysis of the mass and heat transfer.

5 ONE-DIMENSIONAL TRANSPORT EQUATIONS FOR IN-BIN GRAIN DRYING

In convective air drying of in-bulk grains, two distinct transport mechanisms occur simultaneously, involving heat transfer from the drying air to the kernels and water transport from the interior of the solid to its surface and eventually to the air through evaporation.

Various mathematical models have been proposed to simulate the in-bin drying grains. Among them, the non-equilibrium models, that assume there is no heat and mass equilibrium between the drying air and the grain bed, consist of a set of four partial differential equations

and several relationships defining the initial and boundary conditions. The system of equations of the non-equilibrium models cannot be analytically solved. In virtue of this, usually some simplifications (no ever justified) are introduced in order to reduce the complexity and computational time (Aregba and Nadeau, 2007). The numerical techniques such as the Finite Elements Method are frequently applied to obtain solutions to the simultaneous moisture and heat diffusion equation describing the in-bin drying process.

The heat and mass transfer rates depend on both temperature and concentration differences as well as on the air velocity field. The governing partial differential equations (PDEs) describing the simultaneous transfer of heat, mass and momentum in two distinct sub-domains (air and solid) during drying of amaranth grains are presented.

The following assumptions were taken into account (Aregba and Nadeau, 2007):

- The volume shrinkage is negligible during the drying process;
- The temperature gradients within the individual kernels are negligible;
- The kernel-kernel conduction is negligible;
- The airflow is plug-type;
- Accumulation terms from energy and mass balances are negligible compared to gradient terms;
- An accurate thin-layer equation and moisture equilibrium moisture content are available;
- Heat and mass transfer are one-dimensional.

Governing equations

One-dimensional (1D), time-dependent equations for heat and mass transfer during deep-bed amaranth drying with axially ascendant flowing air (y-direction) were derived, based on the following heat and mass balances for air and grain (Lund, 2009).

- Mass transfer equation for grains:

$$q_{Vm} = (1-\varepsilon)\rho_g \frac{6h_{mef}}{D_{eq}}\left(\overline{M} - M_e\right)$$

(53)

$$(1-\varepsilon)\rho_g\left(\frac{\partial \overline{M}}{\partial t}\right) = -q_{Vm}$$

(54)

$$\text{or,} \quad \frac{\partial \overline{M}}{\partial t} = -6\frac{h_{mef}}{D_{eq}}\left(\overline{M} - M_e\right)$$

(55)

- Mass transfer equation for air:

$$\wp_a\left(\frac{\partial o_m}{\partial t} + V_a\frac{\partial o_m}{\partial y}\right) = q_{Vm}$$

(56)

- Heat transfer equation for air:

$$q_V = (1-\varepsilon)\frac{6h}{D_{eq}}\left(T_a - T_g\right)$$

(57)

$$\wp_a\left(\frac{\partial(C'_{pa}\,T_a)}{\partial t} + V_a\frac{\partial(C'_{pa}T_a)}{\partial y}\right) = -q_V + u_m q_{Vm}$$

(58)

$$\text{or,} \quad \varepsilon \rho_a \frac{D_a C_{pa}' T_a}{\partial t} = \frac{6(1-\varepsilon)}{D_{eq}} \left\{ h(T_g - T_a) + u_m \rho_g h_{mef} (\overline{M} - M_e) \right\} \tag{59}$$

- Heat transfer equation for grain:

$$(1-\varepsilon)\rho_g \left(\frac{\partial (C_{pg}' T_g)}{\partial t} \right) = q_V - u_m q_{Vm} - (1-\varepsilon)\rho_g \, hfg \, \frac{\partial \overline{M}}{\partial t} \tag{60}$$

$$\text{or,} \quad \rho_g \left(\frac{D_{ef} C_{pa}' T_g}{\partial t} + hfg \, \frac{\partial \overline{M}}{\partial t} \right) = \frac{6}{D_{eq}} \left\{ h(T_a - T_g) - u_m \rho_g h_{mef} (\overline{M} - M_e) \right\} \tag{61}$$

where q_{Vm}: volumetric moisture transfer (mol/(s m^3)): q_V: volumetric heat transfer (W/m^3); $u_m = u_{m0} + C_{pm}(T_g - T_{m0})$ internal energy of moisture (J/kg); u_{m0}: internal energy of moisture at the reference temperature T_{m0} (J/kg); T_a: air temperature (K); T_g: grain temperature (K).

Boundary and initial conditions

- Boundary conditions for momentum balance equation were as follows:

At the inlet flow: $u = V_a$; At the outlet flow: $\partial u / \partial y = P = 0$ (62)

- Initial conditions for air humidity and temperature, grain moisture content and temperature were written as follows:

At $t=0$: $o_m = o_{m0}$; $T_a = T_{a0}$; $\overline{M} = M_0$; $T_g = T_{g0}$ (63)

- Boundary conditions for air humidity and temperature in the inlet bed section (y=0):

$o_m = o_{min}$; $T_a = T_\infty$ (64)

- Boundary conditions for air humidity and temperature in the outlet bed section (y=L):

Convective flux $\quad n \cdot (-D_a \nabla o_m) = 0 \quad$ or, $\quad \frac{\partial o_m}{\partial y} = 0$ (65)

Convective flux $\quad -n \cdot (-k_a \nabla T_a) = 0 \quad$ or, $\quad \frac{\partial T_a}{\partial y} = 0$ (66)

- Boundary conditions for moisture content and temperature of grain in the kernel surface were:

$$-D_{ef} \frac{\partial \overline{M}}{\partial y} = h_{mef} (\overline{M} - M_e) \tag{67}$$

$$-k_g \frac{\partial T_g}{\partial y} = h(T_g - T_a) \tag{68}$$

where o_{m0}: initial air humidity (kg water-vapor/kg air); T_{a0}: initial air temperature (°C); T_{g0}: initial grain temperature (°C); o_{min}: air humidity at the inlet (y=0, bed bottom); T_{ain}: air temperature at the inlet (y=0, bed bottom); n: normal to kernel surface.

Domain definition and discretization

The bed height of grains (0.18 m) was regarded to define the dimensional domain, which was discretized by 96 Lagrange quadratic elements (Fig. 7, scaled up to 0.18 m), considering increasing element length from the base to the top of the grain bed. The effect of the mesh density on the convergence of results was checked.

One-Dimensional Transport Equations for Moisture Mass, Heat and Momentum Transfer in both phases (solid and gas) were solved using the following Application Modes of COMSOL Multiphysics® 3.5a: transient analysis of Convection and Diffusion (for air and grain) from Multitphysics Module; transient analysis of General Heat Transfer (for air and grain) from the Heat Transfer Module; and state analysis of fluid flow with Darcy´s Law (for air) from the Earth Science Module.

The grain bed was considered like unique material with effective properties. The above described experimental data and relationships of thermo-physical properties, equilibrium moisture content, heat of sorption, drying kinetics and resistance to airflow were used to define the Constants, Scalar and Global Expressions in the definition of the COMSOL model. Physical properties, transfer coefficients, voids fractions and superficial velocities were specified, and pressure-drops through the grain bed, and rates of heat and mass transfer from the kernels to the air, were determined.

Model resolution

The results show the reduction in kernel moisture with time and along the length of the column, and the increase of the air humidity ratio. As example, the following graphs show the spatial-temporal profiles of air and kernel temperature (Figs. 9 and 10), air relative humidity (Fig. 11) and grain moisture content (Fig. 12) during drying of amaranth grains with 12% d.b. initial moisture content and 15°C initial grain temperature, in a deep-bed of 0.18 m, dried with air at 45°C, 10% relative humidity, 0.11 m/s airflow rate.

Figure 13 presents the mean moisture content of the bed of grains at 16.7 hours of drying reaching a uniform humidity of about 10.3% d.b.; while the extrusion plot of the Fig. 14 shows the traveling wave pattern (Lund, 2009) in the equilibrium (surface) moisture along the drying process.

Finally, Fig. 15 exhibits the pressure drop (or airflow resistance) that suffer the air when going through the grain bed.

Figs. 9 and 10 display the air and grain temperature profiles obtained by simulation at distances 0.01 m from the bottom of the grain bed, up to a bed depth of 0.18 m. These curves show enthalpy gain grains at the expense of air cooling. As the grain is heated and loses moisture, this moisture by transferred to inter granular air, increasing its relative humidity during its passage through the bed, as shown in Fig. 11.

It can be noted that the grain immediately in contact with the drying air quickly reaches the thermal equilibrium with the inlet air. While, the following layers –exposed to an airflow with driving force lost- are increasing their temperature more and more slowly, since the air loses enthalpy while ascending through the grain bed.
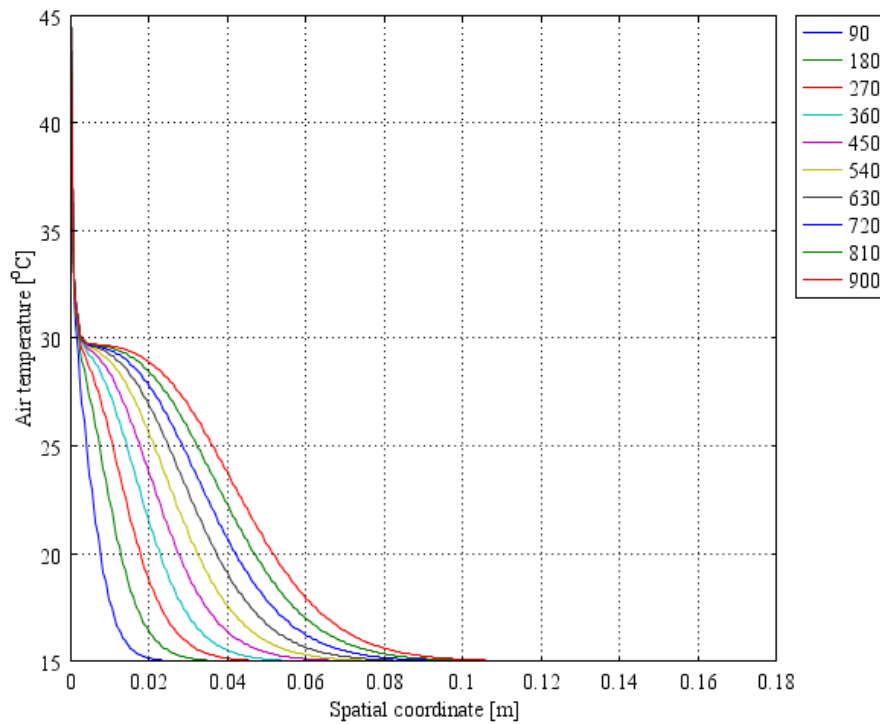
Figure 9. Simulated spatial profiles of air temperature at different drying times (range: 90−900 s) for in-bin amaranth drying at the conditions: M_0=12% d.b.; T_{g0}=15 °C; ε=0.4; rh_{in}=0.1; T_{ain} =45ºC; V_a=0.11 m/s.
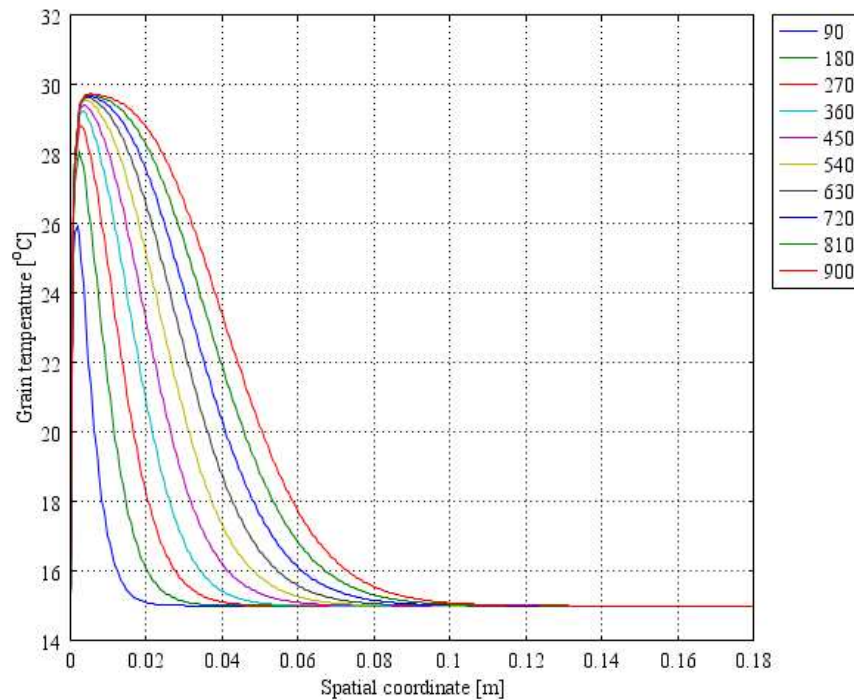
Figure 10. Simulated spatial profiles of grain temperature at different drying times (range: 90−900 s) for in-bin amaranth drying at the conditions: M_0=12% d.b.; T_{g0}=15 °C; ε =0.4; rh_{in}=0.1; T_{ain} =45ºC; V_a=0.11 m/s.
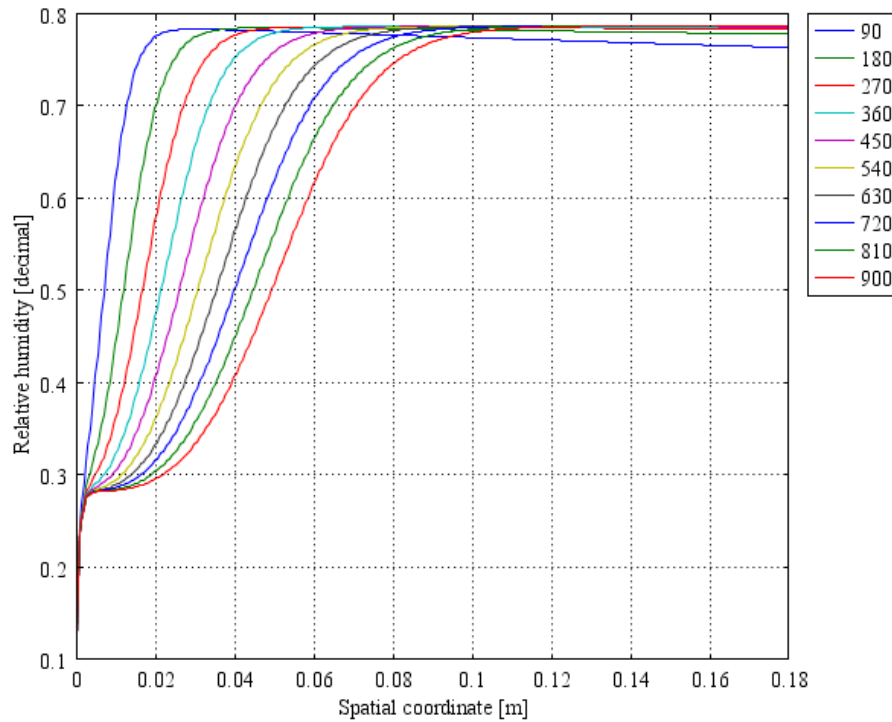
Figure 11. Simulated spatial profiles of air relative humidity at different drying times (range: 90−900 s) for in-bin amaranth drying at the conditions: M_0=12% d.b.; T_{g0}=15 ºC; ε=0.4; rh_{in}=0.1; T_{ain}=45ºC; V_a=0.11 m/s.
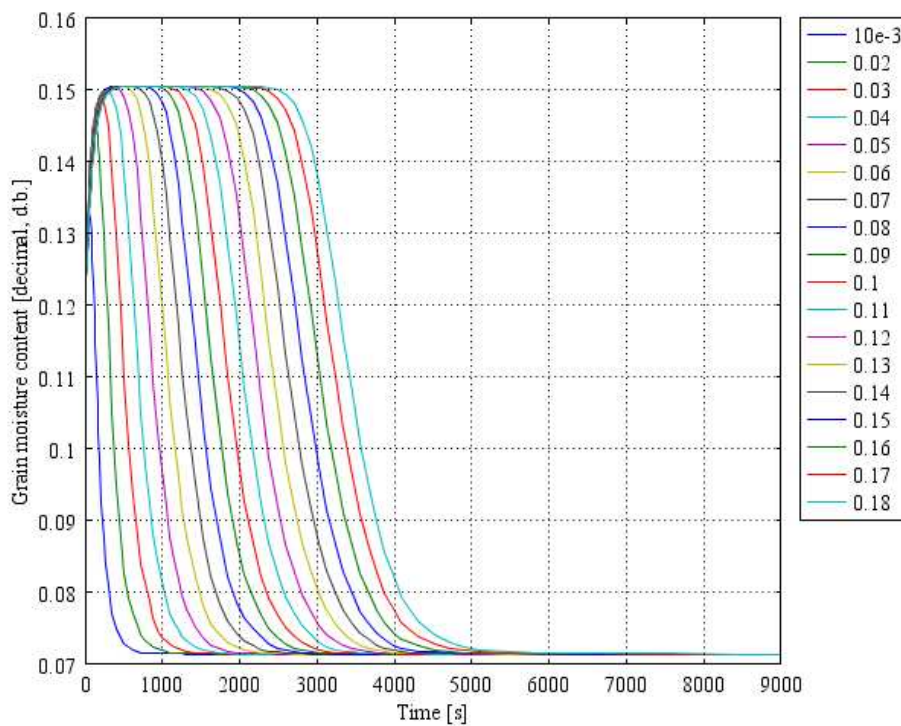
Figure 12. Simulated temporal profiles of grain moisture content at different bed depths (range: 0.1−0.18 m) for in-bin amaranth drying at the conditions: M_0=12% d.b.; T_{g0}=15 ºC; ε=0.4; rh_{in}=0.1; T_{ain} =45ºC; V_a=0.11 m/s.
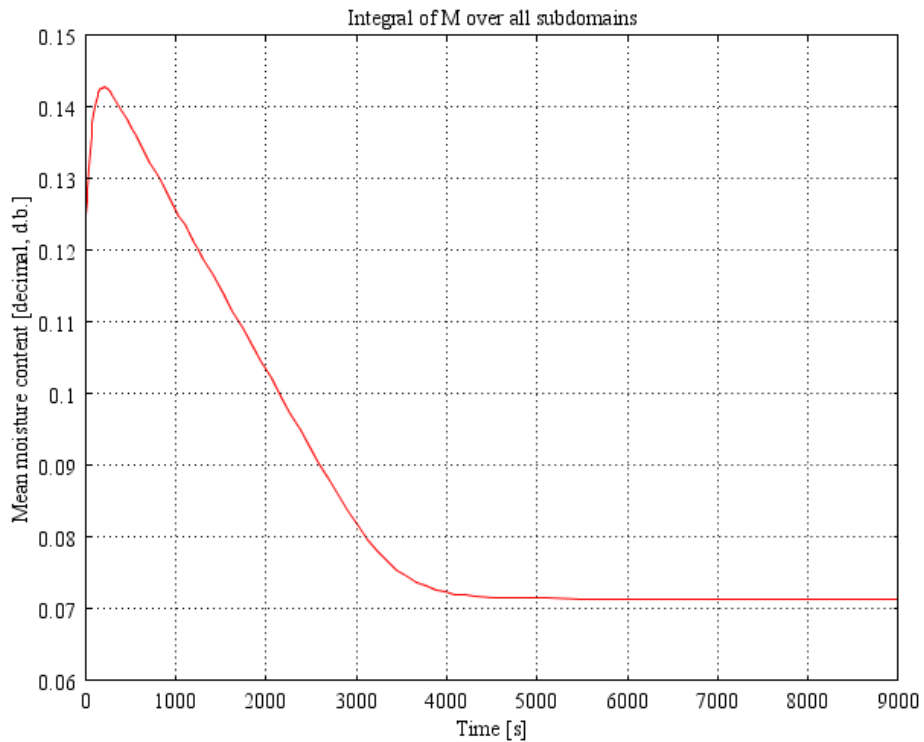
Figure 13. Simulated mean moisture content profile for in-bin amaranth grains drying at the conditions: L=0.18 m; M_0=12% d.b.; T_{g0}=15 ℃; ε=0.4; rh_{in}=0.1; T_{ain} =45℃, V_a=0.11 m/s.
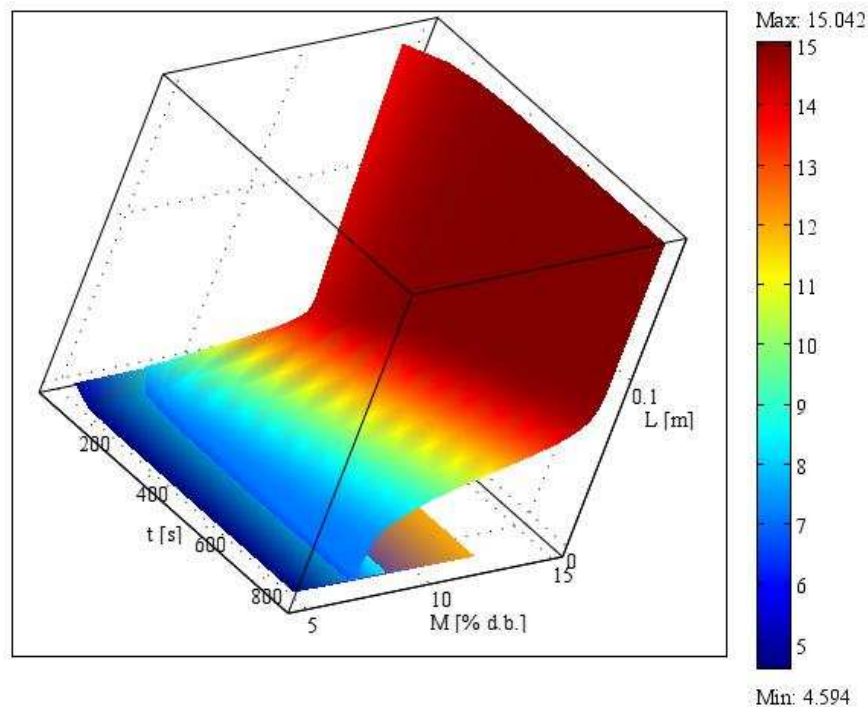
Figure 14. Simulated moisture traveling wave across the deep-bed of amaranth grains during drying at the conditions: L=0.18 m; M_0=12% d.b.; T_{g0}=15 ℃; ε=0.4 ; rh_{in}= 0.1; T_{ain} =45℃, V_a=0.11 m/s.
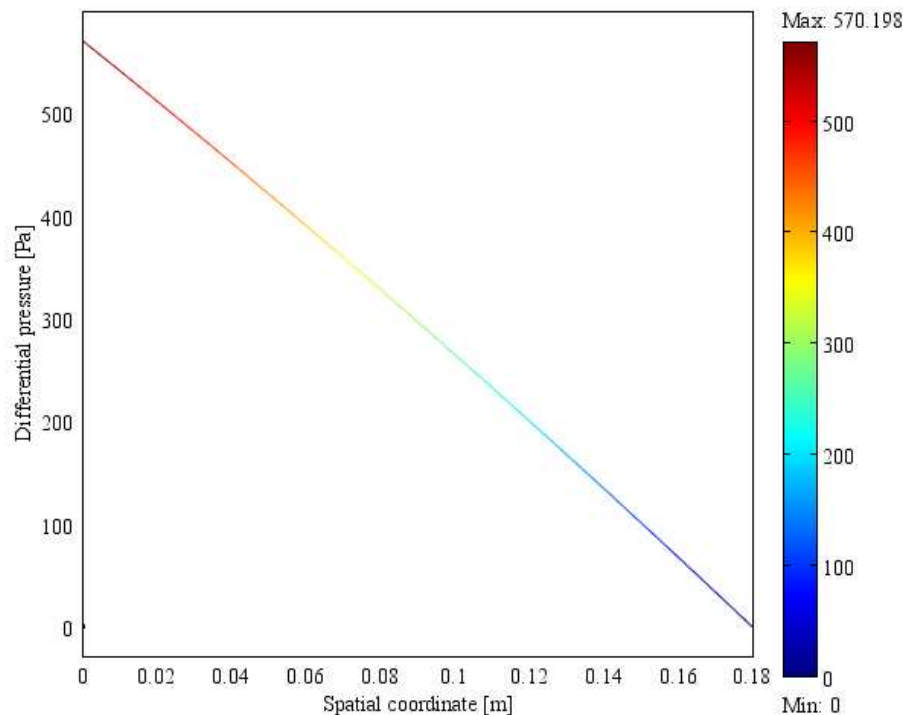
Figure 15. Simulated spatial profile of pressure drop of in-bin amaranth grains during drying/aeration at the conditions: L=0.18 m; M_0=12% d.b.; T_{g0}=15 ºC; ε=0.4 ; rh_{in}=0.1; T_{ain} =45ºC, V_a=0.11 m/s.

Moisture profiles in Fig. 12 show the gradual change of moisture content of grains along the bed depth during drying. Grains near the air inlet quickly reach equilibrium moisture sorption with the drying air, which draws the moisture into the upper moistening at the beginning of the process. Then, the drying process proceeds layer by layer being reached in each of them the equilibrium of moisture content at the local temperature and relative humidity.

As result of this, there is a distribution of moisture and grain temperature along the bed depth (in the same way that there is a distribution of relative humidity and air temperature surrounding the grain inter granular locally). Figure 13 shows the volumetric average bed moisture content obtained through the integration of all subdomains in the bed volume; sorption equilibrium is reached in about 4000 s. Under these conditions, a pressure drop per unit of bed depth of about 2418 Pa/m –usually called resistance to airflow- occurs across the passing of air through the bed depth of 0.18 m (Fig. 15).

All these simulations of the FEM model provided useful information about the grain moisture reduction varying in time and spatially along the length of the silo.

6 CONCLUSIONS

The transport phenomena involved in amaranth grain drying/aeration process were analyzed. A general predictive model for deep-bed grain drying, based on validated models of a single-kernel drying kinetic and airflow resistance, was formulated.

A new single-kernel amaranth drying model was constructed, and solved with COMSOL Multiphysics to predict the simultaneous heat and mass transfer during drying. The generated numerical data from the single-kernel model corresponding to the volumetric average moisture content of grain and its time derivative were correlated. A moisture transfer model

per unit volume was applied to a deep-bed of kernels with specified porosity.

The in-bin drying model allowed predicting moisture, temperature and pressure profiles by coupling the classical transport equations to the virtual work principle, written in terms of the balances of mass, heat and momentum.

Solutions of the one-dimensional in-bin grain drying showed the evolution of changes in moisture and heat transfer, which can be useful in the design of dryers.

REFERENCES

Abalone, R., Cassinera, A., Gastón, A., and Lara, M.A., Some physical properties of amaranth seeds. Biosystems Engineering, 89(1):109–117, 2004.

Abalone, R., Cassinera, A., Gastón, A. and Lara, M.A., Thin layer drying of amaranth seeds. Biosystems Engineering, 93(2):179–188, 2006.

Aregba, A.W., and Nadeau, J.P., Comparison of two non-equilibrium models for static grain deep-bed drying by numerical simulations. Journal of Food Engineering, 78:1174–1187, 2007.

Becker, H.A., A study of diffusion in solids of arbitrary shape with application to the drying of the wheat kernel. Journal of Applied Polymer Science, 1(2):212–226, 1959.

Brooker, D.B., Bakker-Arkema, F.W., and Hall, C.W., Drying and Storage of Grains and Oil Seeds. Chapman & Hall, New York, 1992.

Choi, Y., and Okos, M.R., Effects of temperature and composition on the thermal properties of foods. Food Engineering and Process Applications, Elsevier Applied Science Publishers, London, 1:93–101, 1986.

Coronel Toro, J.F., Colección de Tablas, Gráficas y Ecuaciones de Transmisión de Calor Versión 3.2. Dpto. de Ingeniería Energética y Mecánica de Fluidos, Universidad de Sevilla, 2005.

Crank, J., The Mathematics of Diffusion. Oxford, University Press, New York, 1964.

Cubillos Varela, A., and Barrero Mendoza, O., Design and implementation of a strategy of predictive control of paddy rice drying. Rev. Fac. Ing. Univ. Antioquia, 56:8–86, 2010.

de Andrade, E.T., Couto, S.M., and de Queiroz, D.M., Distribuição da pressão estática em uma coluna de canola: Análise por elementos finitos. Revista Brasileira de Engenharia Agrícola e Ambiental, 5(2):288–295, 2001.

Fortes, M., Martins, J.H., Pinheiro Amantéa, R., and Romero Ferreira, W., Transient and spatial energy and exergy analysis of deep-bed corn drying. Paper from the "State-of-the-Art in Application of Finite Element Numerical Solutions to Engineering Problems: A Session Honoring Pioneering Contributions of Professor Kamyar Haghighi", American Society of Agricultural and Biological Engineers (www.asabe.org), Reno, Nevada, 2009.

Garg, D., Maier, D.E., Modeling non–uniform airflow distribution in large grain silos using Fluent. Proceedings of the 9th International Working Conference on Stored Product Protection. Campinas (SP), Brazil, PS7-12–6158, 2006.

Gavrila, C., Ghiaus, A.G., and Gruia, I., Heat and mass transfer in convective drying processes. Excerpt from the Proceedings of the COMSOL Conference 2008, Hannover, Canada, 2008.

Haghighi, K., and Segerlind, L.J., Modeling simultaneous heat and mass transfer in an isotropic sphere-a finite element approach. Transactions of the ASAE, 31(2):629–637, 1988.

Holman, J.P., Heat Transfer, 4th Edition McGraw-Hill, New York, 1976.

Ibarz-Ribas, A., and Barbosa-Cánovas, G.V., Operaciones Unitarias en la Ingeniería de Alimentos. Colección Tecnología de Alimentos. Editorial Mindi-Prensa, Barcelona, España,

2005.

Jia, C., Mathematical modeling and glass transition mapping for rice drying in a cross-flow dryer. Transactions of the ASAE. Paper Number 02-6073, pp. 2–7, 2002.

Lague, L., and Jenkins, B.M., Modeling pre-harvest stress cracking of rice kernels, Part 2: Implementation and use of the model. Transactions of the ASAE, 34(4):1812–1823, 1991.

Li, C., Grain Amaranth. University of Kentucky, Cooperative Extension Service, College of Agriculture, CDBREC Crop Profiles, 2011.

López, A. Transmisión de calor por convección. Correlaciones para la convección forzada. http://lopezva.wordpress.com/, 2011.

Lund, K.O., A moisture transfer model for drying of grain. Proceedings of the COMSOL Conference, Boston, 2009.

Martinello, M.A., Muñoz, D.J., and Giner, S.A., Mathematical modeling of low temperature drying of maize: Comparison of numerical methods for solving the differential equations. Biosystem Engineering, 114:187–194, 2013.

Masciarelli, R., Stancich, S., and Stoppani, F., Unidad Nº 2: Transferencia de Materia, Universidad Tecnológica Nacional, Facultad Regional Rosario, 30 págs., 2012.

Milojevića, D.Ž., and Stefanović, M.S., Convective drying of thin and deep beds of grain. Chemical Engineering Communications, 13(4-6):261–269, 1982.

Mujica Sánchez, A., Izquierdo, J., Marathee, J.P., Morón, C., and Jacobsen, S.V., Memorias de la Reunión Técnica y Taller de Formulación de Proyecto Regional sobre Producción y Nutrición Humana en Base a Cultivos Andinos, Lima, Perú, 1999.

Pagano, A.M., and Mascheroni, R.H., Isosteric heat of water vapor sorption of Amaranthus cruentus L. seeds, Proceedings IV Congreso Iberoamericano de Ingeniería de Alimentos *“CIBIA IV”*, Valparaíso, Chile, 2003a.

Pagano, A.M., and Mascheroni, R.H., Isotherms of equilibrium sorption for amaranth grains. *Proceedings IV Congreso Iberoamericano de Ingeniería de Alimentos “CIBIA IV”*, Valparaíso, Chile, 2003b.

Pagano, A.M., and Mascheroni, R.H., Water sorption of Amaranthus cruentus L. seeds modelled by GAB equation. International Journal of Food Properties, 6(3):369–391, 2003c.

Pagano, A.M., and Mascheroni, R.H., Sorption isotherms for amaranth grains. Journal of Food Engineering, 67(4):441–450, 2005.

Pagano, A.M., and Mascheroni, R.H., Técnicas de optimización basadas en elementos finitos para el diseño del flujo de fluidos en lechos porosos. Aplicación a la aireación de granos de amaranto. Congreso Argentino de Ingeniería Química (ISSN 1850-3500/3519, Latindex 3004/2260), 6:1–18, 2010.

Pagano, A.M., and Mascheroni, R.H., Modeling simultaneous heat and mass transfer in an amaranth grain during drying: A finite element approach. Mecánica Computacional (ISSN 166-6070, Latindex 12316), 30:1645–1668, 2011.

Ronoh, E.K., Kanali, C.L., Mailutha, J.T., and Shitanda, D., Modeling thin layer drying of amaranth seeds under open sun and natural convection solar tent dryer. Agricultural Engineering International: the CIGR Ejournal, Manuscript 1420, Vol. XI, 13 pages, 2009.

Sabarez, H.T., Computational modelling of the transport phenomena occurring during convective drying of prunes. Journal of Food Engineering, 111:279–288, 2012.

Stakić, M., Banjac, M., and Urošević, T., Numerical study on hygroscopic material drying in packed bed. Brazilian Journal of Chemical Engineering, 28(2):273–284, 2011.

Sun, Y., Pantelides, C., and Chalabi, Z., Mathematical modelling of near-ambient grain drying. Computers and Electronic in Agriculture, 13:243–271, 1995.

Thompson, T.L., Pearl, R.M., and Foster, G.H., Mathematical simulation of corn drying – A

new model. Transactions of the ASAE, 11(4):582–586, 1968.

Wang, D.C., and Fon, D.S., Applications of MATLAB-based software to drying simulation. Keynote Lecture of Seventh Conference "Process integration, modelling and optimisation for energy saving and pollution reduction" PRES 2004, Prague, Czech Republic, 2004.

Wu, B., Yang, W., and Jia, C., A three-dimensional numerical simulation of transient heat and mass transfer inside a single rice kernel during the drying process. Biosystems Engineering, 87(2):191–200, 2004.

Zare, D., Jayas, D.S., and Singh, C.B., A generalized dimensionless model for deep bed drying of paddy. Drying Technology, 30:44–51, 2012.